

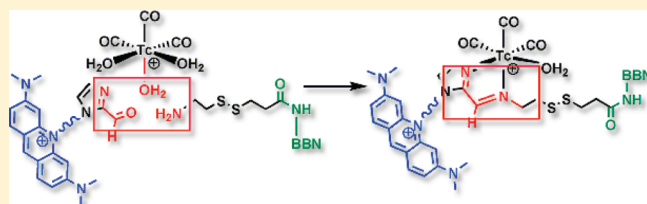
Metal Complex Mediated Conjugation of Peptides to Nucleus Targeting Acridine Orange: A Modular Concept for Dual-Modality Imaging Agents

Karel Zelenka,[†] Lubor Borsig,[‡] and Roger Alberto^{*,†}

[†]Institute of Inorganic Chemistry and [‡]Institute of Physiology, University of Zürich, Winterthurerstrasse 190, 8057 Zürich, Switzerland

S Supporting Information

ABSTRACT: To target the nucleus of specific cells, trifunctional radiopharmaceuticals are required. We have synthesized acridine orange derivatives which comprise an imidazole-2-carbaldehyde function for coordination to the $[\text{Re}(\text{CO})_3]^+$ or $[\text{}^{99\text{m}}\text{Tc}(\text{CO})_3]^+$ core. Upon coordination, this aldehyde is activated and rapidly forms imines with amines from biological molecules. This metal-mediated imine formation allows for the conjugation of a nuclear targeting portion with a specific cell receptor binding function directly on the metal. With this concept, we have conjugated the acridine orange part to a bombesin peptide directly on the $^{99\text{m}}\text{Tc}$ core and in one step. In addition, a linker containing an integrated disulfide has been coupled to bombesin. LC/MS study showed that the disulfide was reductively cleaved with a 60 min half-life time. This concept enables the combination of a nucleus targeting agent with a specific cell receptor molecule directly on the metal without the need of separate conjugation prior to labeling, thus, a modular approach. High uptake of the BBN conjugate into PC-3 cells was detected by fluorescence microscopy, whereas uptake into B16BL6 cells was negligible.



INTRODUCTION

Molecular imaging modalities such as single photon emission computed tomography (SPECT) and positron emission tomography (PET) are major methods for noninvasive diagnosis of organ malfunctions or diseases.¹ Over the past years, the combination of different imaging modalities has become a major focus in advanced imaging. By using different regions of the electromagnetic spectrum for imaging, complementary information about, e.g., physiology and metabolism of particular sites in cells or even in entire organisms may be received concertedly.^{2,3} Combination of SPECT or PET and CT, for instance, is at the stage of clinical routine and allows for combining radionuclide distribution in tissue with anatomical information.^{4,5} Although both SPECT and PET have achieved millimeter resolution, it would be desirable to combine either of these two methods with optical imaging techniques. Luminescence-based imaging allows at least on the *in vitro* level following in real time the compound in the intracellular space. Highly accurate sensing allows assessment of the particular intracellular compartment in which the compound accumulates. Numerous examples for fluorescence imaging appeared in the literature with organic or metal-based fluorescence markers.^{6–11} Ideally, optical imaging would also be possible *in vivo*; however, many fluorescence markers are not suitable for deep-body penetration visualization of biological events. *In vitro* optical imaging does allow, however, localization of a compound on the subcellular level. This is particularly important if a diagnostic or therapeutic radionuclide-based agent is designed to target a particular cell compartment such as the cell

nucleus. Confirmation of compound accumulation in the target is preferentially received from optical imaging since this modality allows nanometer resolution in cells. *In vitro* knowledge about site specificity of a compound can then be extended to the second modality, namely, *in vivo* radioimaging. For a successful combination of optical and radioimaging, chemical identification of the cold, luminescent, and radioactive compound is mandatory. An increasing number of publications are emphasizing the importance of single-compound-based dual-modality imaging based on a combination of subcellular luminescence and *in vivo* imaging from γ -emission.^{12–14} One main strategy to target nuclei of living cells with radiolabeled compounds is based on conjugation of a suitable chelator to NLS (nucleus localizing signal) peptides.¹⁵ Such cell and nucleus penetrating peptides can carry various molecules such as simple metal complexes,¹⁶ peptides, proteins, antisense PNA, or plasmid DNA¹⁷ or are labeled with radioisotopes to quantify *in vitro* and *in vivo* biodistribution.^{18–22}

In our own endeavors to target the nucleus of specific cells, we combined $^{99\text{m}}\text{Tc}$ as a favorable SPECT radionuclide with fluorescence markers such as acridine orange or pyrene.^{21,23} The rationale behind these studies is to benefit from the Auger electrons of $^{99\text{m}}\text{Tc}$ to double-strand break DNA of, e.g., cancerous cells.^{24–26} Along this strategy, a bioconjugate consists of a nuclear targeting agent (with luminescence properties) and a cell

Received: January 14, 2011

Revised: March 15, 2011

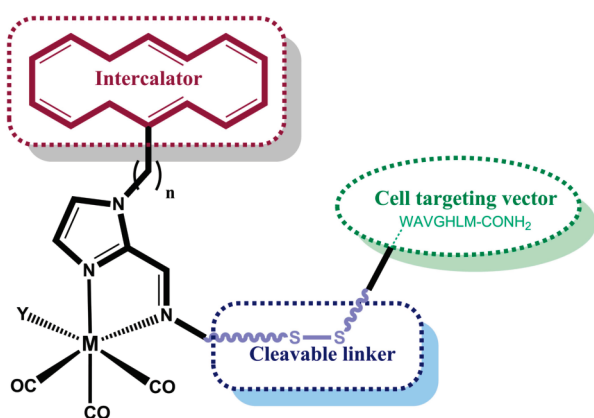
Published: April 12, 2011

receptor specific compound such as a peptide (Scheme 1). The peptide moiety (e.g., bombesin) targets cells with a specific, strongly (over)expressed receptor (GRP receptor for bombesin). Active, receptor-mediated uptake results in site-specific accumulation of the conjugate. Degradation of the peptide in lysosomes sets the intercalator (fluorescent marker) free, which often exhibits strong interaction with and uptake into the DNA. Such fluorescent carriers enhance the accumulation of complexes in the cell nucleus. Optionally, a cleavable linker ensures the cleavage of the receptor targeting agent from the nucleus targeting complex. This bifunctional bioconjugate is then radiolabeled for *in vivo* imaging (Scheme 1).

The synthesis of such constructs is demanding, and any new combination entails a new “total synthesis” of DNA targeting agent, cell receptor specific moiety, and chelator. Lengthy procedures are not very convenient for efficient drug finding or development. Conjugating these two principles directly on the SPECT imaging modality (^{99m}Tc) introduces an *in situ* building block concept. The metal complex fragment does mediate the conjugation of the nuclear targeting and the cell targeting molecules. Accordingly, each individual vector can be replaced without the need of new additional syntheses.

We present in this study the metal-mediated conjugation of a nuclear targeting agent (violet in Scheme 1) with cell receptor targeting peptides (green) and model molecules. In this approach, the aldehyde coordinates to the $[\text{Re}(\text{OH}_2)_3(\text{CO})_3]^+$ moiety. The

Scheme 1. Concept of a Cell-Specific, Nuclear Targeting Trifunctional Bioconjugate



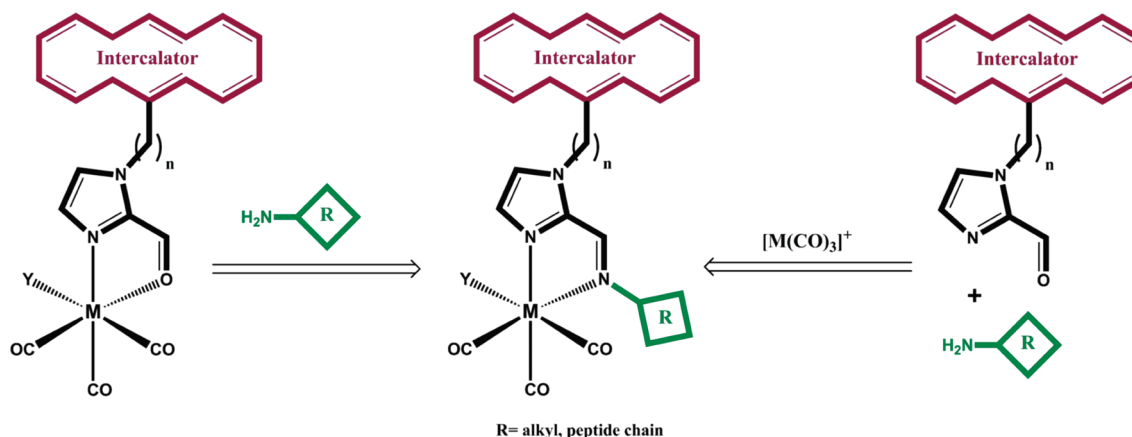
activated aldehyde is susceptible for imine formation with the H_2N -terminus of a peptide (Scheme 2). Fluorescence microscopy studies confirm highly selective uptake of this bioconjugate in the targeted cells.

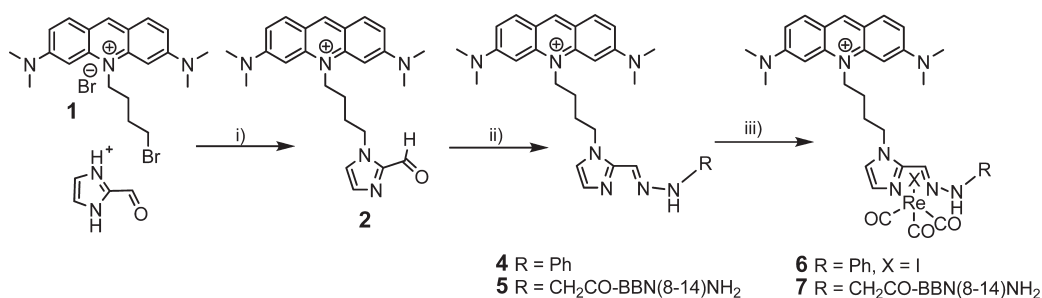
RESULTS AND DISCUSSION

Syntheses. In the building block approach, the combination of a nucleus targeting function and a cell targeting vector is bound to the $[\text{Re}(\text{OH}_2)_3(\text{CO})_3]^+$ core via a bidentate imine or hydrazone chelator. The *in situ* formation of these bidentate ligands from an amine and aldehyde represents the base for the building block concept, since each part can be altered while maintaining an identical synthetic procedure. The resulting complex is cationic and of the general form $[\text{Re}(\text{OH}_2)(\text{L}^2)(\text{CO})_3]^+$. An anion replaces the coordinated water ligand, yielding an overall neutral complex. Due to its strongly fluorescent properties, we have selected acridine orange (AO) as the intercalating nucleus targeting agent and imidazole-2-carboxyaldehyde (ima) as bidentate ligand. We and others have shown previously that heteroaromatic aldehydes are strong ligand groups for coordination to the $[\text{Re}(\text{OH}_2)_3(\text{CO})_3]^+$ moiety.^{27–31} Compound **1** was prepared according to a published procedure³² followed by alkylation of the imidazole-2-carboxyaldehyde to yield **2** in reasonable yield. Coupling of a hydrazine model compound gave the corresponding hydrazone **4**, which now contains a strong bidentate chelator. Reaction with $[\text{Re}(\text{OH}_2)_3(\text{CO})_3]^+$ in methanol/water gave the model complex **6**. Complex **7** which contains both the nucleus targeting agent and a receptor-specific bombesin peptide (BBN) was prepared similarly. The reaction of **2** with the bombesin peptide **3** afforded the hydrazone **5**. Subsequent addition of $[\text{Re}(\text{OH}_2)_3(\text{CO})_3]^+$ gave the complex **7**. Complex **7** is now a model for trifunctional radiopharmaceuticals and comprises the nucleus targeting agent, the cell targeting vector, and the metal center (Scheme 3). Since the hydrazones **4** and **5** are water stable, they can directly be subjected to labeling studies.

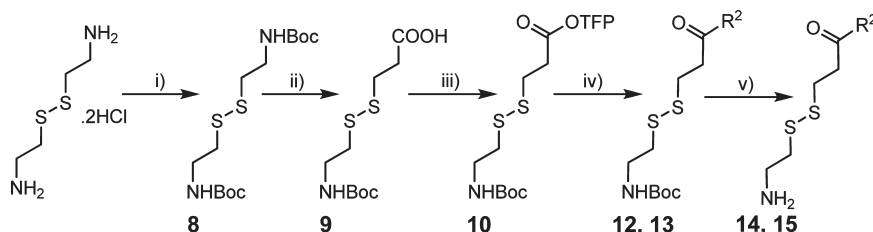
A further building block for a final conjugate is the cleavable linker. Disulfide bonds are known to be cleaved by thiols via thiol/disulfide exchange.³³ They are frequently used in prodrug designs for pharmaceuticals. In the intracellular space, they are cleaved by reduction with GSH which sets the active drug free.^{34–36} For our purposes, the disulfide containing cleavable linker **10** was prepared

Scheme 2. Building Block Concept for the Metal-Mediated Formation of Cell-Specific, Nucleus Targeting Radiopharmaceuticals

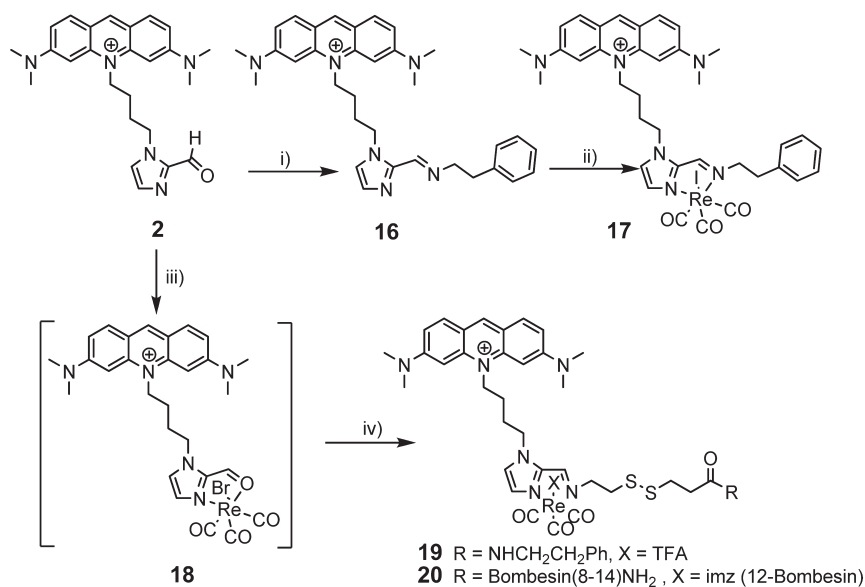


Scheme 3^a

^a (i) K₂CO₃, DMF; (ii) phenyl-hydrazine, EtOH or 3, PBS; (iii) [Re(OH₂)₃(CO)₃]⁺, KI, MeOH/H₂O or MeCN/PBS.

Scheme 4. Synthesis of the Orthogonal, Disulfide-Based Cleavable Linker 10 and Its Conjugate to a Peptide 15^a

^a (i) Boc₂O, NaOH, dioxane/water; (ii) HSCH₂CH₂COOH, Et₃N, CHCl₃; (iii) DIPC, TFP, DMF; (iv) Et₃N, DMF; (v) TFA/CH₂Cl₂. 12, 14: R = NH(CH₂)₂Ph; 13, 15: R² = -BBN(8-14)NH₂.

Scheme 5^a

^a (i) PhCH₂CH₂NH₂, MgSO₄, CHCl₃; (ii) [Re(OH₂)₃(CO)₃]⁺, KI, MeOH/PBS; (iii) [Re(OH₂)₃(CO)₃]⁺, H₂O; (iv) 14 or 15 PBS, MeCN.

in a three-step synthesis. The amino groups of cysteamine were BOC-protected to give **8**. Thiolytic cleavage of the disulfide with mercaptopropionic acid afforded the acid **9**. The activated TFP ester **10** for coupling to terminal amines was prepared along standard procedures. The TFP ester **10** was then used for the preparation of compounds **12** and **13**. The free amines **14** and **15** were obtained after BOC deprotection (Scheme 4).

Hydrazone such as **4** or **5** are relatively stable toward hydrolysis, but imines are not. The model complex **17** was first prepared

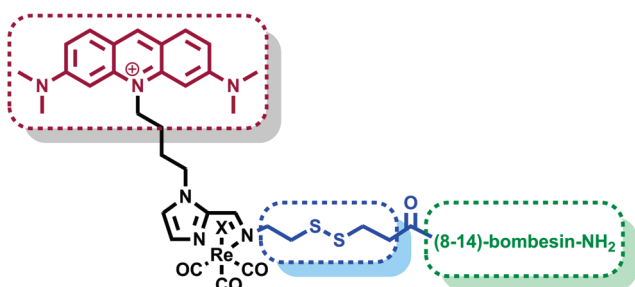
by the reaction of imine **16** with [Re(OH₂)₃(CO)₃]⁺. Isolation of the free imines from the reaction of the aldehyde **2** with **14** or **15** was not possible due to their fast hydrolysis. To receive the true trifunctional compounds **19** and **20**, the aldehyde **2** was reacted in water with an excess of [Re(OH₂)₃(CO)₃]⁺. The orange compound **18** precipitated from solution. In **18**, the aldehyde is coordinated to the rhenium center. ¹H NMR confirmed the presence of the coordinating aldehyde rather than a coordinated semiacetal.²⁷

Compound **18** is the key model compound for labeling reactions and therefore for the metal-mediated assembly of two different types of targeting agents. Compound **18** reacted with **14** or **15** under imine formation to give the trifunctional compounds **19** and **20**, respectively (Scheme 5). Important for the later labeling with ^{99m}Tc , the complexes **19** or **20** were also obtained from a “one-pot” reaction. Compound **2**, **14**, or **15** together with $[\text{Re}(\text{OH}_2)_3(\text{CO})_3]^+$ was dissolved in a MeOH/PBS mixture (1:1). After 12 h at 50 °C, compound **19** or **20** could be purified by preparative HPLC chromatography. The yields after purification for both procedures were comparable.

Complex **20** now comprises the nucleus targeting agent, the cell targeting vector with a disulfide cleavable linker, and the metal center (Scheme 6).

Ideally, complete complex **20** is taken up by the cell through receptor-mediated endocytosis, thus ensuring cell specificity. Inside the cell, the disulfide linker is cleaved with the reduced form of GSH, cleaving the peptide vector from the metal-nucleus targeting moiety complex. Since the remaining complex is relatively small, it can permeate the nuclear membrane without necessity of active transport. Intercalation with DNA proved to be a key process for accumulation of such conjugates in the cell nucleus.²⁴ The cleavage of the disulfide bond also prevents the exclusion of the complex from the cell through a receptor. The

Scheme 6. Complex 20 Comprising Nucleus Targeting Agent (Red), Cell Targeting Vector (Green) with a Disulfide Cleavable Linker (Blue), and Hexacoordinated Metal Center



trifunctional complexes **19** and **20** are rhenium-based and can be used for fluorescence imaging (see later). Fluorescence microscopy allows for following the biological pathways of these compounds on the subcellular level, whereas the ^{99m}Tc homologues can be used for *in vivo* imaging. The unprecedented advantage of this building block principle is the fact that not only **14** and **15** but principally any amines can be selected to complete the trifunctional conjugates. Coordination of the aldehyde in **2** to the $[\text{Re}(\text{CO})_3]^+$ center activates the carbonyl carbon. Although nucleophilic attack of water competes for imine formation, once formed, the imine complex (e.g., **17**) is so strong that the reaction is irreversible and runs to completion. This is crucial for the ^{99m}Tc experiments, since quantitative formation of the radiopharmaceutical is mandatory.

Cleavage Studies. Compounds **19** and **20** comprise the disulfide-cleavable linker which is expected to be reduced in the intracellular space and to release the nucleus targeting function. *In vitro* studies should elucidate rate and mechanism of glutathione GSH-mediated cleavage of the disulfide bond. Compound **19** (in PBS) was added to a freshly prepared GSH solution (in PBS). The final concentrations of the GSH and complexes were 0.5 mM and 0.01 mM, respectively. This GSH concentration is normally found in cells.³⁷ The solution was incubated at 37 °C and samples were taken every 26 min and analyzed with HPLC-MS (see Supporting Information). Figure 1 shows the progress of the cleavage reaction. The integrated chromatograms of total ion counts (TIC) of one of the cleavage products (**21** m/z : 515.3 $[\text{M}]^+$) is plotted versus the starting materials (sum of the intensities of **19** m/z 1066.4 $[\text{M}]^+$, **19a** m/z 988.4 $[\text{M-TFA+Cl}]^+$, and **19b** m/z 476.7 $[\text{M-TFA}]^{2+}$ are plotted). Compounds **19a** and **19b** are formed in solution via slow anion exchange and change over time.

The TIC of complex **22a** (m/z : 781.3 $[\text{M}]^+$, major product) exhibits the same growing trend as **21**. The different physico-chemical properties of **22a** influenced the MS measurement (ion trapping, ejection, and detection). The maximum of the **22a** signal was about three times below the trace of **21**. The disulfide bridge in **19** can be cleaved by GSH on the peptide side, resulting in **21**, or on the complex side resulting in **24**. HPLC-MS evidenced that the formation of undesired **24** (or **24a** and **24b**

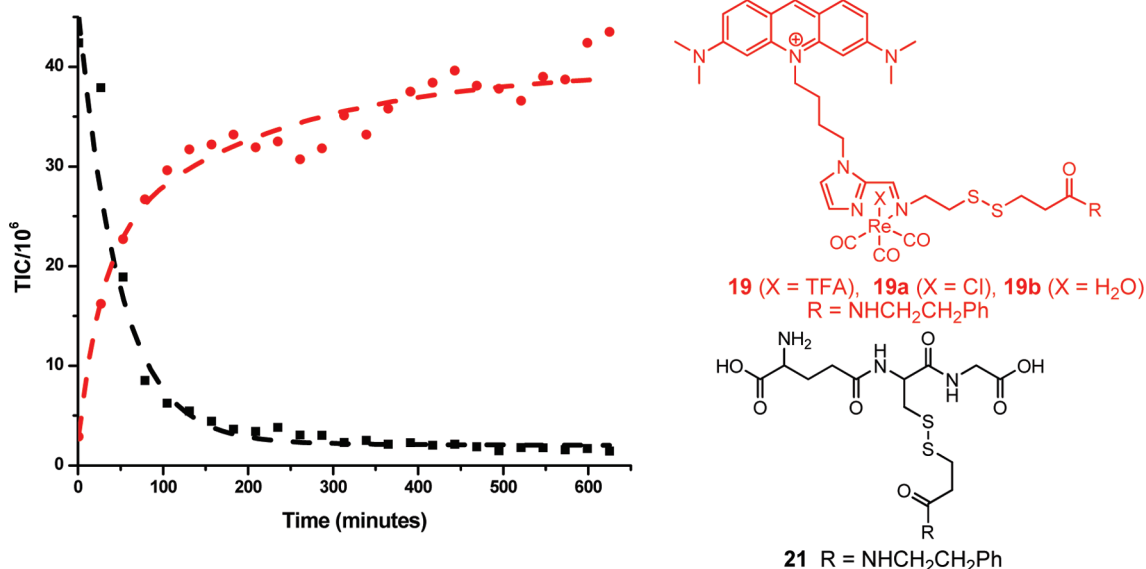


Figure 1. Plot of the time dependence of TIC intensities of **21** (red line) and **19** (sum of **19**, **19a**, and **19b**; black line).

Scheme 7. Cleavage Products after Reaction of 18 or 19 with GSH

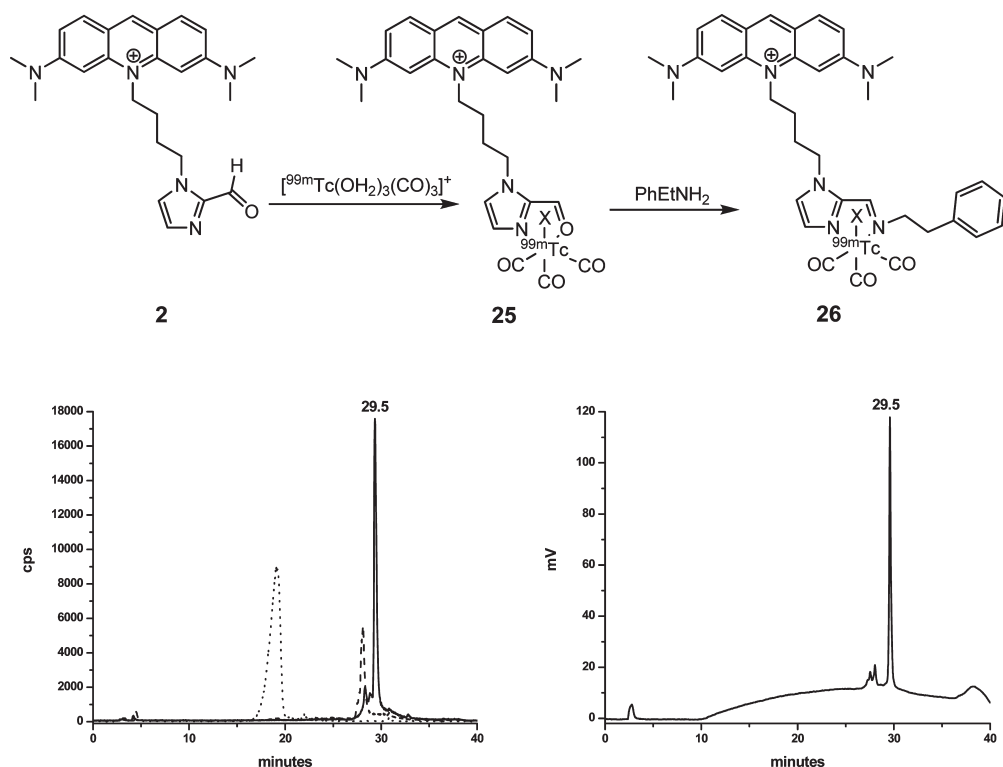
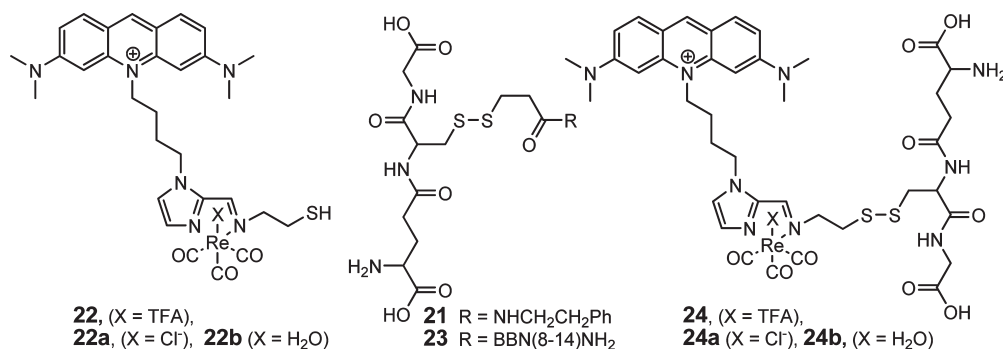


Figure 2. Left: radioactive HPLC traces of $[\text{}^{99\text{m}}\text{Tc}(\text{OH}_2)_3(\text{CO})_3]^+$ (dotted line), **25** (dashed line), and **26** (solid line). Right: UV-vis trace of corresponding Re complex **17a** (X = Cl⁻; see ESI); Gradient D.

after exchange of X) was negligible as compared to **22a** or **21**. The half-life of disulfide cleavage with the GSH was about 60 min. Due to “steady state” intracellular GSH concentration,^{37,38} cleavage inside the cells could be even faster. A similar study was done with complex **20**. The formation of the cleavage products **22a** and **23** displayed similar trends as for **19** (Figure 1). An overview for the cleavage products is given in the Scheme 7.

$^{99\text{m}}\text{Tc}$ -Labeling Studies. The precursor $[\text{}^{99\text{m}}\text{Tc}(\text{OH}_2)_3(\text{CO})_3]^+$ was prepared from $[\text{}^{99\text{m}}\text{TcO}_4]^-$ according to literature procedures or with the commercially available Isolink kit (Covidien, Tyco-Mallinckrodt Med. B.V. Petten, NL).^{39,40} It should be emphasized that $^{99\text{m}}\text{Tc}$ concentrations are in the range of 10^{-6} to 10^{-9} M. After preparation, the solution was buffered with 0.1 M phosphate buffer to pH 7.4. Conversions to products were quantified by HPLC analyses with γ -detection. Reaction times, concentrations, and temperature varied.

Depending on the ligand, the synthesis of complexes of the general type $[\text{}^{99\text{m}}\text{Tc}(\text{X})(\text{L}^2)(\text{CO})_3]^+$ can be done in one or two steps. Solvent or an anion X is coordinated to the sixth available coordination site on the *fac*- $[\text{}^{99\text{m}}\text{Tc}(\text{CO})_3]^+$. Labeling was first tested with a model amine and amino acids under various conditions to confirm the feasibility of the process with $^{99\text{m}}\text{Tc}$. The preparation of complex **26** was done in two steps. The reaction of aldehyde **2** (0.1 mM, 30 min, 90 °C) with $[\text{}^{99\text{m}}\text{Tc}(\text{OH}_2)_3(\text{CO})_3]^+$ (Figure 2, $R_t = 19.2$ min dotted line) gave the intermediate **25** (dashed line, $R_t = 28$ min). After addition of the phenylethylamine (0.2 mM), the mixture was heated to 90 °C for 45 min to yield the complex **26** ($R_t = 29.5$ min, solid line). The same result was also obtained from the “one-pot” preparation, mixing all components together and heating at 90 °C for 45 min. The formation of complex **26** was confirmed by comparing the retention time of with the Re analogue **17a** (Figure 2, also see ESI).

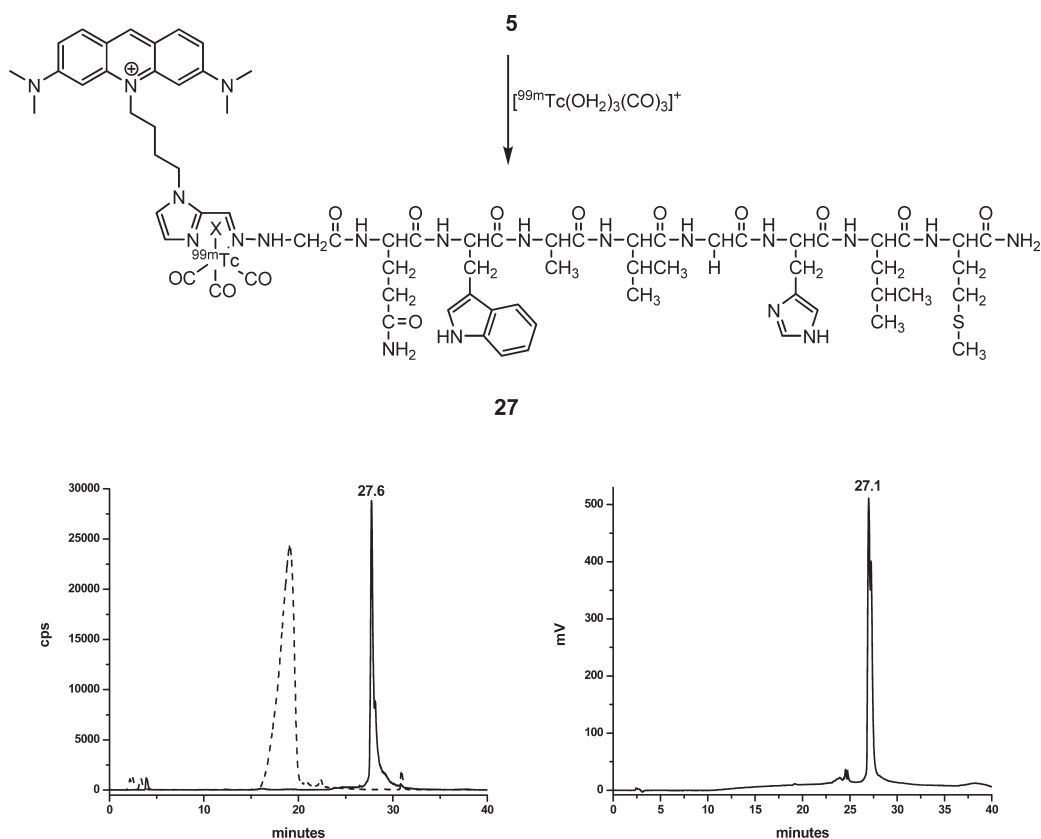


Figure 3. Left: radioactive HPLC traces of $[^{99\text{m}}\text{Tc}(\text{OH}_2)_3(\text{CO})_3]^+$ (dashed line) and **27** (solid line). Right: UV trace of corresponding Re complex **7** (Gradient D).

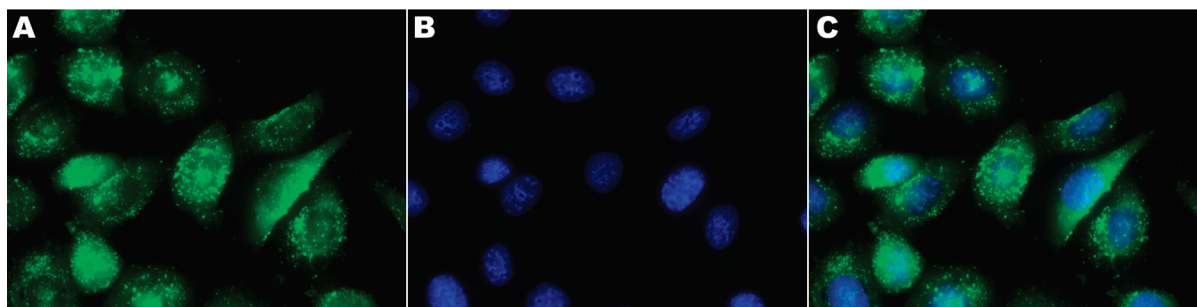


Figure 4. Uptake of the complex **20** into PC-3 cells by fluorescence microscopy. Cells were incubated with $20\ \mu\text{M}$ complex **20** for 6 h, washed, then an additional 18 h in the fresh medium, followed by fixation of cells and nuclear staining by DAPI. (A) PC-3 cells, loaded with **20** in the cytoplasm (green), clear structured staining. (B) DAPI staining of nucleus (blue). (C) Merged image (overlay).

The same approach was used to prepare the $^{99\text{m}}\text{Tc}$ analogue of **20**. However, even by variation of gradients and solvents, the aldehyde complex **25** and resulting imine complex (**25** + **15**) were hardly distinguishable and displayed comparable retention times. For detailed labeling study and comparison with corresponding Re complex **20**, see ESI. The labeling of **5** ($0.22\ \text{mM}$) with $[^{99\text{m}}\text{Tc}(\text{OH}_2)_3(\text{CO})_3]^+$ at $90\ ^\circ\text{C}$ after 60 min provided product **27** with a retention time of 27.6 min (Figure 3, solid line).

Cell Uptake Studies. We selected a human prostate adenocarcinoma cell line, PC-3, which does express the GRP receptor and B16-BL6 mouse melanoma cell line with little or no expression of the GRP receptor. The cell uptake of complex **20** was monitored in the green fluorescence filter as described in the

Experimental Section. To localize the compound in the cell, we stained nuclei with DAPI (4',6-diamidino-2-phenylindol), routinely used in cell biology. The PC-3 cells were exposed to **20** ($20\ \mu\text{M}$) and the uptake was followed by fluorescence microscopy (Figure 4). Complex **20** clearly accumulated in the cell. Green fluorescence was mainly detected in the cytoplasm, exhibiting substructured distribution, probably in lysosomes. There is no enhanced accumulation of fluorescence in the nucleus. Complex **7** was studied in a similar manner to **20**. The accumulation in the cell was also observed with comparable intensities to those for **20**.

The trifunctional complex **20** contains the cell-specific vector (truncated 8–14 BBN peptide). Thus, only cells with the corresponding receptor should accumulate **20**. To confirm such a specific uptake, cell studies were performed on a B16-BL6

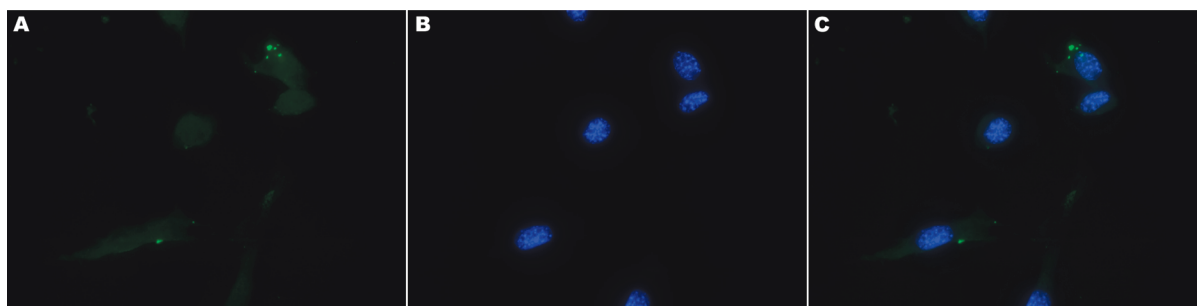


Figure 5. Uptake of complex **20** by B16BL6 cells, performed as described for PC-3. (A) Green channel image. (B) DAPI nucleus staining (blue). (C) Merged image (overlay).

mouse melanoma cell line which does not express the GRP receptor. The difference between the PC-3 (Figure 4) and B16BL6 (Figure 5) is significant. While PC-3 cells were loaded with **20** in the cytoplasm, there was virtually no accumulation in the B16BL6 cell line. The uptake of complex **20** by PC-3 cells was consistent with the presence of the GRP receptor, indicating a receptor-mediated uptake.³²

CONCLUSIONS

The efficient development of imaging probes containing a therapeutic modality demands a flexible building block concept. Herein, we presented an approach in which the conjugation of a nucleus targeting part with a cell-specific vector is metal-mediated, yielding a trifunctional diagnostic and potentially therapeutic radiopharmaceutical. A disulfide-based cleavable linker was introduced on the cell receptor targeting part. *In vitro*, the disulfide linker was cleaved with GSH at a reasonable rate. Fluorescence microscopy with rhenium analogues using GRP/non-GRP expressing cell lines confirmed the cell specificity concept. However, studies with complex **20** did not display increased uptake in the nucleus but stained mainly substructures of the cytoplasm for so far unknown reasons. Detailed cell studies with the trifunctional complex **20** and similar systems, prepared according to the presented building block concept, are currently under investigation. The approach represents a very general method for the *in situ* preparation of strong bidentate ligands and its use for further development of functional multimodality systems.

EXPERIMENTAL SECTION

General Information. The commercially available reagents were used as received without further purification. Analytical thin-layer chromatography (TLC) was carried out with aluminum-based plates (silica gel 60 F₂₅₄) from Merck. Plates were visualized under UV light ($\lambda = 254$ nm). Flash chromatography was carried out on Flashmaster Solo (Argonaut) by using Merck silica gel 60 (0.040–0.063 mm). Samples were applied as almost saturated solutions in the appropriate solvent. ¹H NMR and ¹³C NMR spectra were performed on a Bruker 400 and 500 spectrometers at 400/500 and 100/125 MHz, respectively. The reported chemical shifts (in δ) are relative to the solvent protons and carbons as a reference. HPLC-MS (ESI) spectra were measured on a Bruker HCT spectrometer with Aquinity UPLC (Waters) with alternating polarity ion detection, using a Macherey-Nagel EC 250/3 Nucleodur C18 Gravity 5 μ m. HPLC solvents were 0.1% formic acid (solvent A) and methanol (solvent B). The gradients used for analyses were as follows:

Gradient A: 0–5 min 90% A, 5–17 min 90–0% A, 17–25 min 0% A, 25–27 min 0–90% A, 27–35 min 90% A, flow 0.3 mL min^{-1} ; Gradient B: 0–2 min 90% A, 2–12 min 90–0% A, 12–17 min 0% A, 17–18 min 0–90% A, 18–25 min 90% A, flow 0.25 mL min^{-1} . HPLC analyses were performed on a Merck L7000 system using a Macherey-Nagel EC 250/3 Nucleodur C18 Gravity 5 μ m for radioactive compounds. HPLC solvents were 0.1% trifluoroacetic acid (solvent A) and MeOH or MeCN HPLC grade (solvent B). Gradient C (MeOH): 0–5 min 90% A, 5–15 min 90–0% A, 15–20 min 0% A, 20–22 min 0–90% A, 22–30 min 90% A. Gradient D (MeCN): 0–5 min 90% A, 5–20 min 90–60% A, 20–23 min 60% A, 23–28 min 0% A, 28–33 min 0% A, 33–34 min 0–90% A, 34–40 min 90% A. Flow rates: 0.5 mL/min, detection with a γ -detector for the radiolabeled compounds. Preparative HPLC was performed on a Varian Pro Star system by using either a Macherey-Nagel VP 250/21 Nucleodur C18 Gravity 5 μ m or a Macherey-Nagel VP 250/40 Nucleosil 100–7 C18 column with a flow rate of 12 mL min^{-1} and 40 mL min^{-1} respectively. The solvents were 0.1% trifluoroacetic acid (solvent A) and methanol or acetonitrile (solvent B).

Cell Culture and Complex Uptake. Human prostate cancer cells, PC-3 were incubated in F12K medium supplemented with 10% fetal calf serum. For microscopy, cells were cultured overnight on four-chamber slides (Nunc) in which ca. 50 000 cells were plated. Next day, cells were washed and fresh media containing complexes **20** or **7** (20 μ m) were added. Cells were incubated with the complex for 6 h. After the loading with a complex, the fresh medium was added and the cells were incubated for additional 18 h, washed with phosphate buffer saline (PBS), and fixed in 4% paraformaldehyde for 10 min in at r.t. After three washings with PBS, cells were incubated in 1 mg mL^{-1} 4',6-diamidino-2-phenylindole (DAPI) for nuclear staining for 10 min at r.t. Cells were washed three times with phosphate-buffered saline (PBS), chambers from the slides were detached, and cells were covered with coverslips in Prolong Mounting medium (Invitrogen). Slides were evaluated on Zeiss Axiovert 200 m with the corresponding fluorescence filters for DAPI ($\lambda_{\text{ex}} = 360$ nm, $\lambda_{\text{em}} = 420$ nm) and acridine orange ($\lambda_{\text{ex}} = 496$ nm, $\lambda_{\text{em}} = 525$ nm).

General Remarks to the Re Complexes. Under common HPLC or HPLC-MS conditions, typically two peaks with a ratio of 1:10 (respectively 1:1 with TFA anion) were observed. The first peak represents the complex, where the anion is replaced with a solvent, while the second peak belongs to the original (whole) complex. During the MS acquisition, the coordinated solvent is usually lost. For complexes containing peptides, the sixth coordination position is probably occupied by imidazole from histidine. Both double- and single-charged species were

observed under HPLC-MS conditions. The elementary analyses were not performed due to the various content of TFA after purification with the preparative HPLC. Thus, to be consistent, the M.W. and concentrations of the compounds were calculated without counterions (e.g., as drawn in the schemes). If not specified in the scheme, the counterions are trifluoroacetates.

3,6-Bis(dimethylamino)-10-(4-(2-formyl-1H-imidazol-1-yl)-butyl)acridinium (2). A suspension of 1H-imidazole-2-carbaldehyde (11 mg, 0.11 mmol) and K_2CO_3 (100 mg, 0.72 mmol) in DMF (10 mL, dry) was stirred at r.t. under N_2 . After 10 min, **1** (70 mg, 0.14 mmol) was added, and the mixture stirred and heated to 50 °C under N_2 . After 16 h, the solvent was removed under HV. The residue was dissolved in 15 mL of CH_2Cl_2 , filtered over Celite, and dried again. Purification by preparative HPLC afforded 36 mg **2** (75%) as an orange powder. 1H NMR (CD_3CN , 400 MHz) δ 9.65 (d, $^3J = 0.8$ Hz, 1H), 8.49 (s, 1H), 7.79 (d, $^3J = 9.3$ Hz, 2H), 7.31 (bs, 1H), 7.18 (d, $^4J = 0.7$ Hz, 1H), 7.14 (dd, $^3J = 9.3$ Hz, $^4J = 2.2$ Hz, 2H), 6.45 (d, $^4J = 1.8$ Hz, 2H), 4.53 (bt, $^3J = 8$ Hz, 2H), 4.43 (t, $^3J = 6.9$ Hz, 2H), 3.20 (s, 12H), 2.07–1.97 (m, 2H), 1.93–1.83 (m, 2H). MS (ESI, Gradient B): t_R 9.3 min; positive mode m/z 448.2 (100) $[M + MeOH]^+$, 416.2 (33) $[M]^+$. MS (ESI) m/z (%) 416.2 (100) $[M]^+$, 448.2(17) $[M + MeOH]^+$; calcd for $C_{25}H_{30}N_5O^+$: 416.24 (100.0).

$NH_2NH_2CH_2CO$ -Bombesin WAVGHLM (3). Truncated hydrazinoacetyl-bombesin **3** (sequence: WAVGHLM) was synthesized SPPS according to the procedure reported previously for hydrazino derivatives of peptides.⁴¹ The product was then purified by reverse-phase HPLC on a preparative C18 column (Macherey-Nagel VP 250/40 Nucleosil 100–7 C18 column), fractions with the peptide were lyophilized, and pure peptide was kept under N_2 in the freezer at –25 °C. **3** was obtained as a white solid. HPLC-MS (ESI, Gradient A): t_R 13.4 min; positive mode m/z 884.5 (100) $[M+H]^+$; calcd for $C_{40}H_{61}N_{13}O_8S$: 883.45 (100.0); negative mode m/z 882.6 (60) $[M-H]^-$, 996.6 (100) $[M+TFA]^-$.

3,6-Bis(dimethylamino)-10-(4-(2-((2-phenylhydrazono)methyl)-1H-imidazol-1-yl)butyl)acridinium (4). The aldehyde **2** (26 mg, 0.062 mmol) was dissolved in the EtOH (1 mL, dry), and phenyl hydrazine (7 mg, 6.3 μ L, 0.062 mmol) was added to the mixture. Reaction was stirred and heated to 80 °C for 4 h; the solvent was then removed in vacuo. The crude product **4** (31 mg, 98%) was pure enough for use in the next step without further purification. 1H NMR (CD_3CN , 400 MHz): δ 10.00 (bs, 1H), 8.42 (s, 1H), 7.94 (s, 1H), 7.70 (d, $^3J = 9.3$ Hz, 2H), 7.12–6.93 (m, 8H), 6.75 (t, $^3J = 7.3$ Hz, 1H), 6.40 (d, $^4J = 1.7$ Hz, 2H), 4.55 (t, $^3J = 7.4$ Hz, 2H), 4.35 (t, $^3J = 6.6$ Hz, 2H), 3.08 (s, 12H), 2.10–2.01 (m, 2H), 2.01–1.92 (m, 2H). HPLC-MS (ESI, Gradient B): t_R 10.8 min; positive mode m/z 506.4 (100) $[M]^+$, $[M+H]^+$ 253.1 (40) $[M+H]^{2+}$; calcd for $C_{31}H_{36}N_7^+$: 506.3 (100).

3,6-Bis(dimethylamino)-10-(4-(2-((2-(Bombesin 8–14)-2-oxoethyl)hydrazono)methyl)-1H-imidazol-1-yl)butyl)acridinium (5). The aldehyde **2** (8 mg, 0.019 mmol) and hydrazino bombesin **3** (25 mg, 0.028 mmol) were dissolved in the PBS (15 mL, pH = 6.5). The mixture was stirred at r.t. under N_2 for 3 days. The orange precipitate was filtered and washed with water and PBS. The crude product was purified by preparative HPLC to give **5** as orange powder in a yield of (12 mg, 48%). HPLC-MS (ESI, Gradient B): t_R 10.0 min; positive mode m/z 641.6 (100) $[M+H]^{2+}$, 1281.7 (75) $[M]^+$; calcd for $C_{65}H_{89}N_{18}O_8S^+$: 1281.7 (100.0).

$[Re(I)(4)(CO)_3]^+$ (6). The hydrazone **4** (8 mg, 0.016 mmol) and KI (50 mg, 0.3 mmol) were dissolved in the methanol/water mixture (6 mL, 2:1), then $[NEt_4]_2[ReBr_3(CO)_3]$ (15 mg, 0.019 mmol) was added. The mixture was stirred 3 h at 60 °C. The solvents were removed in vacuo, and the crude product was purified by preparative HPLC to give **6** as dark orange powder in a yield of (7 mg, 49%). 1H NMR ($DMSO-d_6$, 400 MHz): δ 10.40 (s, 1H), 8.77 (s, 1H), 8.57 (s, 1H), 7.90 (d, $^3J = 9.4$ Hz, 2H), 7.59 (d, $J = 1.4$ Hz, 1H), 7.45 (d, $J = 1.4$ Hz, 1H), 7.24 (dd, $^3J = 9.4$ Hz, $^4J = 2.0$ Hz, 2H), 7.18–7.12 (m, 2H), 7.05–7.00 (m, 3H), 6.54 (bs, 2H), 4.78–4.63 (m, 2H), 4.32 (t, $^3J = 6.6$ Hz, 2H), 3.20 (s, 12H), 2.03–1.93 (m, 2H), 1.77–1.67 (m, 2H). HPLC-MS (ESI, Gradient B): t_R 12.8 min; positive mode m/z 904.3 (100), 902.3 (58) $[M]^+$; calcd for $C_{34}H_{36}IN_7O_3Re^+$: 904.15 (100.0), 902.15 (57.0).

$[Re(5)(CO)_3]^+$ (7). To a solution of **5** (10 mg, 0.007 mmol) dissolved in the acetonitrile/PBS mixture (4 mL, 1:1, pH = 7.4), $[NEt_4]_2[ReBr_3(CO)_3]$ (20 mg, 0.026 mmol) was added. The mixture was stirred under N_2 at 40 °C. After 2 d, the solvents were removed and the crude product purified by preparative HPLC to give **7** as orange powder in a yield of (4 mg, 33%). HPLC-MS (ESI, Gradient B): t_R 11.2 min; positive mode m/z 776.4 (100) $[M]^{2+}$, 1551.5 (10) $[M-H]^+$; calcd for $C_{68}H_{89}N_{18}O_{11}ReS^{2+}$: 1552.62 (100.0).

N,N' -Bis-tert-butoxycarbonylcystamine (8). Compound **8** was prepared according to the published procedure and the analysis was similar to the literature.⁴²

3-((2-(tert-Butoxycarbonylamino)ethyl)disulfanyl)propanoic acid (9). Compound **9** was prepared according to the published procedure⁴³ using the 3-mercapto propanoic acid instead of 2-mercaptoacetic acid. 300 mg (yield 30%) of the acid **9** were obtained. TLC $R_f = 0.26$ ($CHCl_3/MeOH$, 9/1). 1H NMR ($CDCl_3$, 400 MHz): δ 4.93 (bs, 1H), 3.46 (bs, 2H), 2.95 (bt, $^3J = 6.9$ Hz, 2H), 2.84–2.77 (m, 4H), 1.46 (s, 9H). MS (ESI) m/z (%) 304.1 (100) $[M + Na]^+$; 316.1(100) $[M + Cl]^-$, 280.4 (90) $[M - H]^-$; calcd for $C_{10}H_{19}NO_4S_2$: 281.08 (100.0).

2,3,5,6-Tetrafluorophenyl 3-((2-(tert-butoxycarbonylamino)ethyl)disulfanyl)propanoate (10). A solution of **9** (170 mg, 0.6 mmol) in DMF (1 mL, dry) was cooled to 4 °C and diisopropylcarbodiimid (93 μ L, 76 mg, 0.6 mmol) was added. The mixture was stirred 15 min under N_2 , and then 2,3,5,6-tetrafluorophenol (100 mg, 0.6 mmol) in DMF (0.5 mL, dry) was slowly added and reaction was stirred at r.t. After 12 h, CH_2Cl_2 (3 mL) was added, precipitate was filtered, and filtrate was evaporated to dryness. Purification by flash chromatography (gradient, hexane to hexane:MTBE 6:1) afforded compound **10** (100 mg, 38%) as a white solid. 1H NMR ($CDCl_3$, 500 MHz) δ 7.05–7.00 (m, 1H), 4.90 (bs, 1H), 3.46 (bd, $^3J = 6.0$ Hz, 2H), 3.13 (t, $^3J = 6.9$ Hz, 2H), 3.05 (t, $^3J = 6.9$ Hz, 2H), 2.83 (t, $^3J = 6.7$ Hz, 2H), 1.45 (s, 9H). MS (ESI) positive mode m/z (%) 452.0 (100) $[M + Na]^+$, 467.9 (80) $[M + K]^+$; negative mode 464.0 (100) $[M + Cl]^-$; calcd 429.07 (100.0). Elemental analysis (%) calcd for $C_{16}H_{19}F_4NO_4S_2$: C 44.75, H 4.46, N 3.26, S 14.93; found C 44.52, H 4.47, N 3.00.

Bombesin WAVGHLM (11). Truncated bombesin **11** (sequence: WAVGHLM) was synthesized SPPS and purified according to the procedure reported previously²⁴.

tert-Butyl 2-((3-oxo-3-(phenethylamino)propyl)disulfanyl)ethylcarbamate.TFA (14). A solution containing **10** (10 mg, 0.023 mmol) and Et_3N (6.4 μ L, 4.7 mg, 0.046 mmol) in 0.3 mL of DMF was stirred for 30 min at room temperature. After addition of 2-phenylethanamine (3.2 μ L, 3.1 mg, 0.025 mmol), the solution

was further stirred for 12 h. The removal of the solvent in vacuo afforded crude product **12**. The residue was dissolved in 1.5 mL of the mixture of dichloromethane–TFA (1:0.5). The mixture was stirred for 3 h under N₂ at r.t. After removal of the solvent in vacuo, the crude product was purified by preparative HPLC to afford 3 mg (31%) of compound **14** as a white solid. ¹H NMR (CDCl₃, 400 MHz): δ 8.31 (bs, 2H), 7.29–7.12 (m, 5H), 6.20 (t, ³J = 5.6 Hz, 1H), 3.46 (q, ³J = 6.5 Hz, 2H), 3.28 (bt, ³J = 5.5 Hz, 2H), 2.94 (bt, ³J = 6.0 Hz, 2H), 2.90 (t, ³J = 6.6 Hz, 2H), 2.77 (t, ³J = 7.0 Hz, 2H), 2.49 (t, ³J = 6.7 Hz, 2H). HPLC-MS (ESI, Gradient B): t_R 10.2 min; positive mode m/z: 285.3 (100) [M+H]⁺; calcd for C₁₃H₂₀N₂O₂: 284.11 (100.0).

Bombesin (15). Truncated bombesin **11** (40 mg, 0.049 mmol, prepared according to the literature) was dissolved in the DMF (dry, 0.5 mL) with Et₃N (20 μL, 15 mg, 0.148 mmol). The mixture was stirred at r.t. under N₂. After 15 min, the solution of **10** (24 mg, 0.056 mmol) in DMF (0.5 mL) was added and mixture was stirred at r.t. under N₂ for 20 h. The solvent was removed in vacuo to afford crude product **13**. The residue was dissolved in 1 mL of the mixture of dichloromethane–TFA (1:1). The mixture was stirred for 12 h under N₂ at r.t. After removal of the solvent in vacuo, the crude product was purified by preparative HPLC to afford 30 mg (62%) of compound **15** as a white solid. HPLC-MS (ESI, Gradient A): t_R 13.8 min; positive mode m/z 975.4 (100) [M+H]⁺, 488.2 (66) [M+2H]²⁺; negative mode m/z 1087.5 (100) [M+TFA]⁻, 973.4 (15) [M-H]⁻; calcd for C₄₃H₆₆N₁₂O₈S₃: 974.43 (100.0).

3,6-Bis(dimethylamino)-10-(4-(2-((phenethylimino)methyl)-1H-imidazol-1-yl)butyl)acridinium (16). 2-Phenylethanamine (6.12 μL, 5.9 mg, 0.048 mmol) was added to the suspension of **2** (8 mg, 0.019 mmol) with dry MgSO₄ (50 mg) in CHCl₃ (1 mL, dry). Reaction mixture was stirred at 60 °C for 12 h, filtered over Celite, and evaporated to dryness to give imine **16** (9.8 mg, 99%). ¹H NMR (CDCl₃, 400 MHz): δ 8.41 (s, 1H), 8.18 (s, 1H), 7.76 (d, ³J = 9.3 Hz, 2H), 7.15–7.08 (m, 3H), 7.08–7.00 (m, 6H), 6.49 (bs, 2H), 4.62 (bt, ³J = 7.8 Hz, 2H), 4.55 (t, ³J = 6.8 Hz, 2H), 3.74 (t, ³J = 7.2 Hz, 2H), 3.22 (s, 12H), 2.76 (t, ³J = 7.2 Hz, 2H), 2.11–2.01 (m, 2H), 1.95–1.84 (m, 2H). MS (ESI) m/z (%) 519.5 (100) [M]⁺; calcd for C₃₃H₃₉N₆⁺: 519.32 (100.0).

[Re(I)(16)(CO)₃]⁺ (17). Imine **16** (10 mg, 0.019 mmol), KI (50 mg, 0.3 mmol), and [NEt₄]₂[ReBr₃(CO)₃] (20 mg, 0.026 mmol) were consecutively dissolved in 4 mL of the mixture of MeOH and PBS (1:1, pH = 6.4). Reaction was stirred for 4 h at 40 °C under N₂. HPLC-MS analysis showed complete product formation. The solvent was removed in vacuo and the product was dried at high vacuum. The crude product was purified by preparative HPLC to afford 8 mg (45%) of compound **17** as a bright orange powder. ¹H NMR (DMSO-*d*₆, 400 MHz): δ 8.94 (s, 1H), 8.78 (s, 1H), 7.90 (d, ³J = 9.4 Hz, 2H), 7.70 (d, ³J = 1.3 Hz, 1H), 7.59 (d, ³J = 1.2 Hz, 1H), 7.24 (dd, ³J = 9.4 Hz, ⁴J = 2.0 Hz, 2H), 7.21–7.14 (m, 4H), 7.10–7.04 (m, 1H), 6.54 (bs, 2H), 4.78–4.73 (m, 2H), 4.36 (t, ³J = 6.8 Hz, 2H), 4.19–4.09 (m, 2H), 3.20 (s, 12H), 3.17–3.07 (m, 1H), 3.06–2.96 (m, 1H), 2.04–1.94 (m, 2H), 1.75–1.64 (m, 2H). MS (ESI, Gradient B): t_R 13.5 min; positive mode m/z 917.2 (100) [M]⁺, 915.2 (56) [M]⁺; calcd for C₃₆H₃₉IN₆O₃Re⁺: 917.17 (100.0), 915.17 (56.7).

[Re(TFA)(14)(CO)₃]⁺ (19). The aldehyde **2** (2 mg, 0.005 mmol) and the [NEt₄]₂[ReBr₃(CO)₃] (10 mg, 0.013 mmol) were dissolved in PBS (2 mL, pH = 6.5). The mixture was stirred and heated under N₂ at 50 °C for 30 min. The formed precipitate was spun down, and supernatant removed. The remaining precipitate was dissolved in the mixture of MeCN:PBS (14 mL, 9:5).

The orange solution was added to the flask containing the amine **14** (3 mg, 0.007 mmol) and the mixture was stirred at r.t. for 16 h; HPLC-MS showed the product formation. The product was purified by preparative HPLC to afford 1 mg (18%) of compound **18** as an orange powder. ¹H NMR (DMSO-*d*₆, 400 MHz): δ 9.09 (s, 1H), 8.77 (s, 1H), 7.94 (t, ³J = 5.5 Hz, 1H), 7.90 (d, ³J = 9.4 Hz, 2H), 7.78 (d, ³J = 1.3 Hz, 1H), 7.58 (d, ³J = 1.2 Hz, 1H), 7.27–7.07 (m, 7H), 6.54 (bs, 2H), 4.75–4.65 (m, 2H), 4.50–4.36 (m, 2H), 4.24–4.14 (m, 1H), 4.14–4.04 (m, 1H), 3.21–2.14 (m, 2H), 3.18 (s, 12H), 3.08–2.91 (m, 2H), 2.70 (t, ³J = 7.0 Hz, 2H), 2.63–2.58 (m, 2H), 2.33–2.28 (m, 2H), 2.11–2.01 (m, 2H), 1.81–1.61 (m, 2H). HPLC-MS (ESI, Gradient B): t_R 12.5 min; positive mode m/z 1066.2 (100) [M]⁺, 1064.3 (60) [M]⁺; calcd for C₄₃H₄₈F₃N₇O₆ReS₂⁺: 1066.26 (100.0), 1064.26 (58.6); t_R 11.0 min; positive mode m/z 476.6 (100) [M-TFA]²⁺; calcd for C₄₁H₄₈N₇O₄ReS₂²⁺: 476.28 (100).

[Re(15)(CO)₃](20)⁺. The aldehyde **2** (4.2 mg, 0.01 mmol) and the [NEt₄]₂[ReBr₃(CO)₃] (22 mg, 0.028 mmol) were dissolved in PBS (5 mL, pH = 6.5). The mixture was stirred and heated under N₂ at 50 °C for 15 min. The formed precipitate was spun down, and supernatant removed. The remaining precipitate was dissolved in the mixture of MeCN:PBS (10 mL, 1:1, pH = 7.4). The orange solution was added to the flask containing the peptide **15** (30 mg, 0.03 mmol) and the mixture was stirred at 66 °C for 24 h. The crude product was purified by preparative HPLC to afford 4 mg (24%) of complex **19** as an orange powder. HPLC-MS (ESI, Gradient A): t_R 15.7 min; positive mode m/z 821.9 (100) [M]²⁺, 1642.4 (50) [M-H]⁺; calcd for C₇₁H₉₄N₁₇O₁₁ReS₃²⁺: 1643.60 (100.0), 1644.61 (75.1).

■ ASSOCIATED CONTENT

S Supporting Information. Detailed materials and methods. This material is available free of charge via the Internet at <http://pubs.acs.org>.

■ AUTHOR INFORMATION

Corresponding Author

*E-mail: ariel@aci.uzh.ch.

■ REFERENCES

- (1) Bartholoma, M. D., Louie, A. S., Valliant, J. F., and Zubieta, J. (2010) Technetium and gallium derived radiopharmaceuticals: comparing and contrasting the chemistry of two important radiometals for the molecular imaging era. *Chem. Rev.* 110, 2903–20.
- (2) Jennings, L. E., and Long, N. J. (2009) ‘Two is better than one’-probes for dual-modality molecular imaging. *Chem. Commun.* 3511–24.
- (3) Louie, A. (2010) Multimodality imaging probes: design and challenges. *Chem. Rev.* 110, 3146–95.
- (4) Mariani, G., Bruselli, L., Kuwert, T., Kim, E. E., Flotats, A., Israel, O., Dondi, M., and Watanabe, N. (2010) A review on the clinical uses of SPECT/CT. *Eur. J. Nucl. Med. Mol. I* 37, 1959–85.
- (5) Marti-Bonmati, L., Sopena, R., Bartumeus, P., and Sopena, P. (2010) Multimodality imaging techniques. *Contr. Media Mol. I* 5, 180–89.
- (6) Puckett, C. A., Ernst, R. J., and Barton, J. K. (2010) Exploring the cellular accumulation of metal complexes. *Dalton Trans.* 39, 1159–70.
- (7) Splith, K., Hu, W. N., Schatzschneider, U., Gust, R., Ott, I., Onambele, L. A., Prokop, A., and Neundorff, I. (2010) Protease-activatable organometal-peptide bioconjugates with enhanced cytotoxicity on cancer cells. *Bioconjugate Chem.* 21, 1288–96.
- (8) Bartholoma, M., Valliant, J., Maresca, K. P., Babich, J., and Zubieta, J. (2009) Single amino acid chelates (SAAC): a strategy for

the design of technetium and rhenium radiopharmaceuticals. *Chem. Commun.* 493–512.

(9) Deshpande, M. S., Kumbhar, A. A., Kumbhar, A. S., Kumbhakar, M., Pal, H., Sonawane, U. B., and Joshi, R. R. (2009) Ruthenium(II) complexes of bipyridine-glycoluril and their interactions with DNA. *Bioconjugate Chem.* 20, 447–59.

(10) Puckett, C. A., and Barton, J. K. (2007) Methods to explore cellular uptake of ruthenium complexes. *J. Am. Chem. Soc.* 129, 46–47.

(11) Puckett, C. A., and Barton, J. K. (2008) Mechanism of cellular uptake of a ruthenium polypyridyl complex. *Biochemistry* 47, 11711–16.

(12) James, S., Maresca, K. P., Babich, J. W., Valliant, J. F., Doering, L., and Zubieta, J. (2006) Isostructural Re and Tc-99m complexes of biotin derivatives for fluorescence and radioimaging studies. *Bioconjugate Chem.* 17, 590–96.

(13) Schaffer, P. J. A. G., Lemon, J. A., Reid, L. C., Pacey, L. K. K., Farncombe, T. H., Boreham, D. R., Zubieta, J., Babich, J. W., Doering, L. C., and Valliant, J. F. (2008) Isostructural fluorescent and radioactive probes for monitoring neural stem and progenitor cell transplants. *Nucl. Med. Biol.* 35, 159–69.

(14) Stephenson, K. A., Banerjee, S. R., Besanger, T., Sogbein, O. O., Levadala, M. K., Mcfarlane, N., Lemon, J. A., Boreham, D. R., Maresca, K. P., Brennan, J. D., Babich, J. W., Zubieta, J., and Valliant, J. F. (2004) Bridging the gap between in vitro and in vivo imaging: isostructural Re and Tc-99m complexes for correlating fluorescence and radioimaging studies. *J. Am. Chem. Soc.* 126, 8598–99.

(15) Miller, A. M., and Dean, D. A. (2009) Tissue-specific and transcription factor-mediated nuclear entry of DNA. *Adv. Drug Delivery Rev.* 61, 603–13.

(16) Noor, F., Kinscherf, R., Bonaterra, G. A., Walczak, S., Wolf, S., and Metzler-Nolte, N. (2009) Enhanced cellular uptake and cytotoxicity studies of organometallic bioconjugates of the NLS peptide in Hep G2 cells. *ChemBioChem* 10, 493–502.

(17) Bendifallah, N., Rasmussen, F. W., Zachar, V., Ebbesen, P., Nielsen, P. E., and Koppelhus, U. (2006) Evaluation of cell-penetrating peptides (CPPs) as vehicles for intracellular delivery of antisense peptide nucleic acid (PNA). *Bioconjugate Chem.* 17, 750–58.

(18) Sarko, D., Beijer, B., Boy, R. G., Nothelfer, E. M., Leotta, K., Eisenhut, M., Altmann, A., Haberkorn, U., and Mier, W. (2010) The pharmacokinetics of cell-penetrating peptides. *Mol. Pharmaceut.* 7, 2224–31.

(19) Zanta, M. A., Belguise-Valladier, P., and Behr, J. P. (1999) Gene delivery: a single nuclear localization signal peptide is sufficient to carry DNA to the cell nucleus. *Proc. Natl. Acad. Sci. U.S.A.* 96, 91–96.

(20) Adam, S. A., and Gerace, L. (1991) Cytosolic proteins that specifically bind nuclear location signals are receptors for nuclear import. *Cell* 66, 837–47.

(21) Häfliger, P., Agorastos, N., Renard, A., Giambonini-Brugnoli, G., Marty, C., and Alberto, R. (2005) Cell uptake and radiotoxicity studies of an nuclear localization signal peptide-intercalator conjugate labeled with [Tc-99m(CO)(3)](+). *Bioconjugate Chem.* 16, 582–87.

(22) Fischer, R., Fotin-Mleczek, M., Hufnagel, H., and Brock, R. (2005) Break on through to the other side - Biophysics and cell biology shed light on cell-penetrating peptides. *ChemBioChem* 6, 2126–42.

(23) Häfliger, P., Agorastos, N., Spingler, B., Georgiev, O., Viola, G., and Alberto, R. (2005) Induction of DNA-double-strand breaks by auger electrons from 99mTc complexes with DNA-binding ligands. *ChemBioChem* 6, 414–21.

(24) Agorastos, N., Borsig, L., Renard, A., Antoni, P., Viola, G., Spingler, B., Kurz, P., and Alberto, R. (2007) Cell-specific and nuclear targeting with [M(CO)(3)](+) (M=Tc-99m, Re)-based complexes conjugated to acridine orange and bombesin. *Chem.—Eur. J.* 13, 3842–52.

(25) Wendisch, M., Freudenberg, R., Drechsel, J., Runge, R., Wunderlich, G., and Kotzerke, J. (2010) Tc-99m reduces clonogenic survival after intracellular uptake in NIS-positive cells in vitro more than I-131. *Nuklearmedizin* 49, 154–60.

(26) Alexandre, A., Tavares, S., and Tavares, J. M. R. S. (2010) *Int. J. Radiat. Biol.* 86, 261–70.

(27) Wang, W. W., Spingler, B., and Alberto, R. (2003) Reactivity of 2-pyridine-aldehyde and 2-acetyl-pyridine coordinated to [Re(CO)(3)](+) with alcohols and amines: metal mediated schiff base formation and dimerization. *Inorg. Chim. Acta* 355, 386–93.

(28) Bourkoulou, A., Paravatou-Petsotas, M., Papadopoulos, A., Santos, I., Pietzsch, H. J., Livaniou, E., Pelecanou, M., Papadopoulos, M., and Pirmettis, I. (2009) Synthesis and characterization of rhenium and technetium-99m tricarbonyl complexes bearing the 4-[3-bromophenyl]quinazoline moiety as a biomarker for EGFR-TK imaging. *Eur. J. Med. Chem.* 44, 4021–27.

(29) Benny, P. D., Fugate, G. A., Barden, A. O., Morley, J. E., Silva-Lopez, E., and Twamley, B. (2008) Metal-assisted in situ formation of a tridentate acetylacetonone ligand for complexation of fac-Re(CO)(3)(+) for radiopharmaceutical applications. *Inorg. Chem.* 47, 2240–42.

(30) Saw, M. M., Kurz, P., Agorastos, N., Hor, T. S. A., Sundram, F. X., Yan, Y. K., and Alberto, R. (2006) Complexes with the fac-{M(CO)(3)}(+) (M=Tc-99m, Re) moiety and long alkyl chain ligands as Lipiodol surrogates. *Inorg. Chim. Acta* 359, 4087–94.

(31) Alvarez, C. M., Garcia-Rodriguez, R., and Miguel, D. (2007) Pyridine-2-carboxaldehyde as ligand: Synthesis and derivatization of carbonyl complexes. *Dalton Trans.* 3546–54.

(32) Zelenka, K., Borsig, L., Alberto, R. (2010). *Org. Biomol. Chem.* Online Early Access. DOI: 10.1039/COB00504E.

(33) Rabenstein, D. L., and Weaver, K. H. (1996) Kinetics and equilibria of the thiol/disulfide exchange reactions of somatostatin with glutathione. *J. Org. Chem.* 61, 7391–97.

(34) Endres, P. J., Macrenaris, K. W., Vogt, S., and Meade, T. J. (2008) Cell-permeable MR contrast agents with increased intracellular retention. *Bioconjugate Chem.* 19, 2049–59.

(35) Ojima, I. (2007) Guided molecular missiles for tumor-targeting chemotherapy a case studies using the second-generation taxoids as warheads. *Acc. Chem. Res.* 41, 108–19.

(36) Satyam, A. (2008) Design and synthesis of releasable folate-drug conjugates using a novel heterobifunctional disulfide-containing linker. *Bioorg. Med. Chem. Lett.* 18, 3196–99.

(37) Meister, A., and Anderson, M. E. (1983) Glutathione. *Annu. Rev. Biochem.* 52, 711–60.

(38) Gilbert, H. F., and Lester, P. (1995) In *Methods in Enzymology*, pp 8–28, Vol. 251, Academic Press, London.

(39) Alberto, R., Schibli, R., Schubiger, A. P., Abram, U., Pietzsch, H. J., and Johannsen, B. (1999) First application of fac-[Tc-99m(OH2)(3)(CO)(3)](+) in bioorganometallic chemistry: design, structure, and in vitro affinity of a 5-HT1A receptor ligand labeled with Tc-99m. *J. Am. Chem. Soc.* 121, 6076–77.

(40) Alberto, R., Ortner, K., Wheatley, N., Schibli, R., and Schubiger, A. P. (2001) Synthesis and properties of boranocarbonate: a convenient in situ CO source for the aqueous preparation of [99mTc(OH2)3(CO)3]+. *J. Am. Chem. Soc.* 123, 3135–36.

(41) Bonnet, D., Grandjean, C., Rousselot-Pailley, P., Joly, P., Bourel-Bonnet, L., Santraine, V., Gras-Masse, H., and Melnyk, O. (2003) Solid-phase functionalization of peptides by an hydrazinoacetyl group. *J. Org. Chem.* 68, 7033–40.

(42) Baugh, S. D. P., Yang, Z., Leung, D. K., Wilson, D. M., and Breslow, R. (2001) Cyclodextrin dimers as cleavable carriers of photo-dynamic sensitizers. *J. Am. Chem. Soc.* 123, 12488–94.

(43) Byk, G., Wetzler, B., Frederic, M., Dubertret, C., Pitard, B., Jaslin, G., and Scherman, D. (2000) Reduction-sensitive lipopolyamines as a novel nonviral gene delivery system for modulated release of DNA with improved transgene expression. *J. Med. Chem.* 43, 4377–87.